Optics Communications 383 (2017) 1–5

Contents lists available at ScienceDirect

Optics Communications

journal homepage: www.elsevier.com/locate/optcom

Enhanced emission in the three-level system of Si and Ge nanostructures

Zhong-Mei Huang [b], Wei-Qi Huang [a,*], Shi-Rong Liu [c], Tai-Ge Dong [a], Gang Wang [a], Xue-Ke Wu [a], Zhi-Rong Han [d], Chao-Jian Qin [b]

[a] Institute of Nanophotonic Physics, Guizhou University, Guiyang 550025, China
[b] State key laboratory of Surface Physics, Key Laboratory of Micro and Nano Photonic Structures (Ministry of Education) and Department of Physics, Fudan University, Shanghai 200433, China
[c] State Key Laboratory of Environmental Geochemistry Institute of Geochemistry, Chinese Academy of Science Institute of Geochemistry, Guiyang 550003, China
[d] School of Mechanical Engineering, Guiyang University, Guiyang 550003, China

ARTICLE INFO

Article history:
Received 10 June 2016
Received in revised form
25 July 2016
Accepted 24 August 2016
Available online 30 August 2016

Keywords:
Three-level system
Quantum dots
Nanolayers
Super-lattice structure

ABSTRACT

Enhanced mission peak near 700 nm is observed on the silicon quantum dots (QDs) embedded in Si amorphous film and the peak near 1100 nm occurs on the silicon nanolayer, which have the emission characteristics of direct band-gap, such as the thresholds effect and the supper-line increasing effect in intensity with pumping in our experiment. It is interesting that the Si QDs embedded in nanosilicon layer are prepared by using pulsed laser deposition (PLD) method after annealing. In the same way, the peak near 900 nm on the Ge QDs and the peak near 1500 nm on the Ge nanolayer are measured in the PL spectra. It is very interesting that the sharper peaks with multi-longitudinal-mode occur in the Si and Ge nanolayers with the super-lattice on SOI in which the QDs are embedded. An emission model for Si and Ge laser on silicon chip with QDs pumping has been provided to explain the experimental results.

The integrated light source on silicon has been challenging to develop due to the indirect band-gap nature of group-IV semiconductors. Persistent efforts in the hope of extending the reach of silicon technology into fully integrated optoelectronic circuit, have been made to achieve efficient light emission from silicon [1–4], meeting the needs for high-bandwidth intra-chip and inter-chip connects. Recently, the Si and Ge nanostructures such as quantum wells (2D) and quantum dots (QDs) have aroused huge scientific interest [5–10], which could transfer the indirect band-gap into direct band-gap or quasi-direct band-gap.

In the letter, it is demonstrated that the nanocrystals of Si and Ge grow in [100] and [111] direction, especially QDs and nanolayers of Si and Ge form after annealing or electron beam irradiation [11], which result in rising of L valley (Ge) and X valley (Si) of conduction band to form direct band-gap. In photoluminescence (PL) spectra, the peak near 700 nm on Si QDs and the peak near the 900 nm on Ge QDs are measured at room temperature. The enhanced peak near 1100 nm in nanolayer involving Si QDs and the peak near 1500 nm in nanolayer involving Ge QDs embedded are measured in the PL spectra. It is very interesting that the characteristic peaks with multi-longitudinal-mode occur in the super-lattice nanolayers involving Si and Ge QDs on silicon on insulator (SOI). An emission model with the QDs pumping and direct band-gap emission has been provided to explain the experimental results, where the shorter lifetime of QDs states is suitable for pumping (the lifetime of QDs states is shorter due to the Heisenberg principle related to $\Delta t \sim h/\Delta E$ in the quantum confinement effect) [12,13]. It is a new way to develop Si and Ge laser on silicon chip.

The silicon wafers of P-type substrate with 10 Ω cm were taken on the sample stage in the fabrication system with nanosecond pulsed laser depositing (PLD) devices as shown in Fig. 1. A nanosecond pulsed Nd:YAG laser (wavelength: 1064 nm, pulse length: 60 ns FWHM, repetition rate: 1000) and a third harmonic of pulsed Nd:YAG laser at 355 nm are used to deposit the Si and Ge nanolayers structure and the super-lattice structure in PLD process in environment of nitrogen or SF_6. It is interesting that the crystal orientation of [100], [110] and [111] can grow up on the amorphous film prepared by PLD process after annealing. Fig. 2(a) shows the TEM image of Si QDs in [100] direction on Si film and their FFT pattern, Fig. 2(b) shows the TEM image of Ge QDs in [111] direction on Si films prepared by PLD process after annealing, and Fig. 2(c) shows the TEM image of Si QDs in the cross-section of silicon nanolayer [14–16].

* Corresponding author.
E-mail address: wqhuang@gzu.edu.cn (W.-Q. Huang).

http://dx.doi.org/10.1016/j.optcom.2016.08.066
0030-4018/

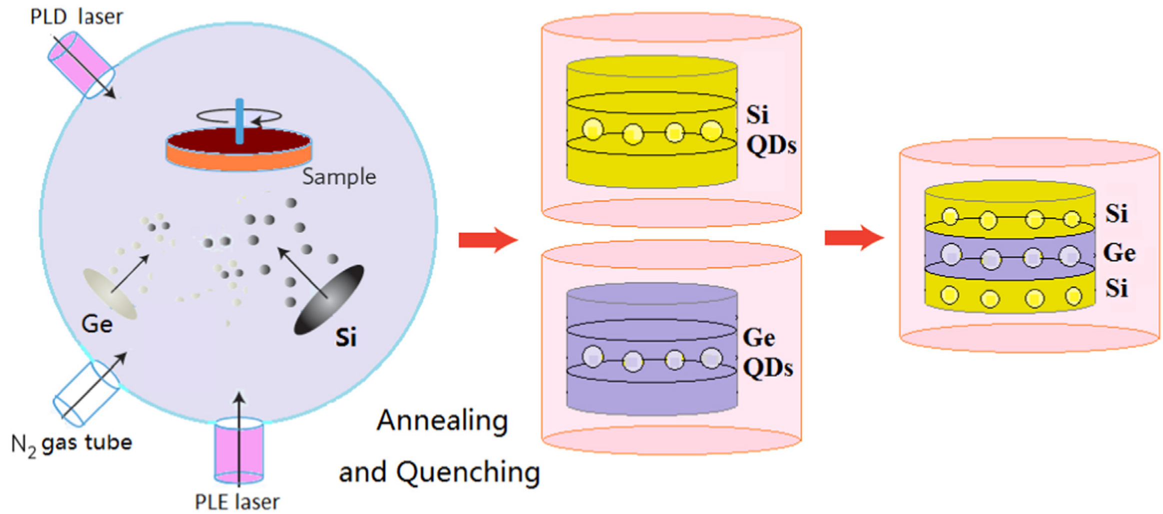

Fig. 1. Fabrication system with PLE and PLD device, in which the Si-Ge layers and the super-lattice structures involving QDs are prepared after annealing and quenching.

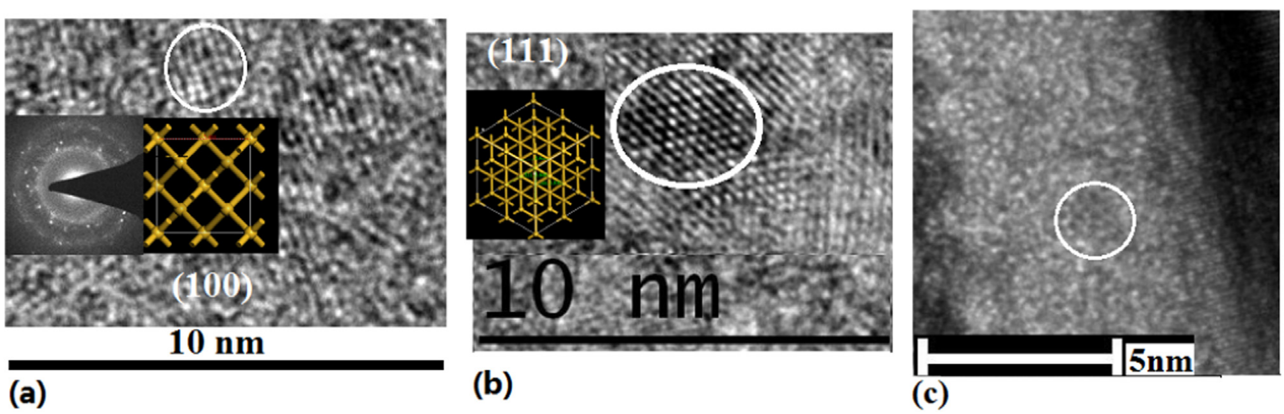

Fig. 2. TEM images of Si-Ge layers involving QDs prepared by PLD process, (a) TEM image of Si QD in [100] direction and FFT pattern as shown in the inset, (b) TEM image of Ge QD in [111] direction, (c) TEM image of Si QD in cross-section of silicon nanolayer.

In the photoluminescence (PL) spectra, the emission peak near 700 nm originates from Si QDs, whose wavelength range is related to the size range of QDs, as shown in Fig. 3(a). And in Fig. 3(b), the PL peak near 900 nm comes from the Ge QDs whose size range is related to the peak width. The relationship between the QDs size and the PL wavelength is confirmed in TEM analysis. Here, the Si QDs are embedded in the thickened layer ($>$ 10 nm).

The PL spectra in silicon nanolayer (5–7 nm) involving Si QDs in [100] direction are measured under the 488 nm excitation in the PL systems at 17 K, as shown in Fig. 4(a), in which the sharper peak at 1154 nm has the emission characteristics of direct band-gap such as the thresholds effect (death region: pumping power $<$ 0.05 W), the supper-linear increasing intensity effect with increase of pumping power (in Fig. 4(b)) and the quenching effect with temperature increase (in Fig. 4(c)). Here, the emission characteristics of the three-level system are observed on the Si QDs embedded in the Si nanolayer, in which the Si QD states play an important role for pumping and the states of the Si nanolayer are

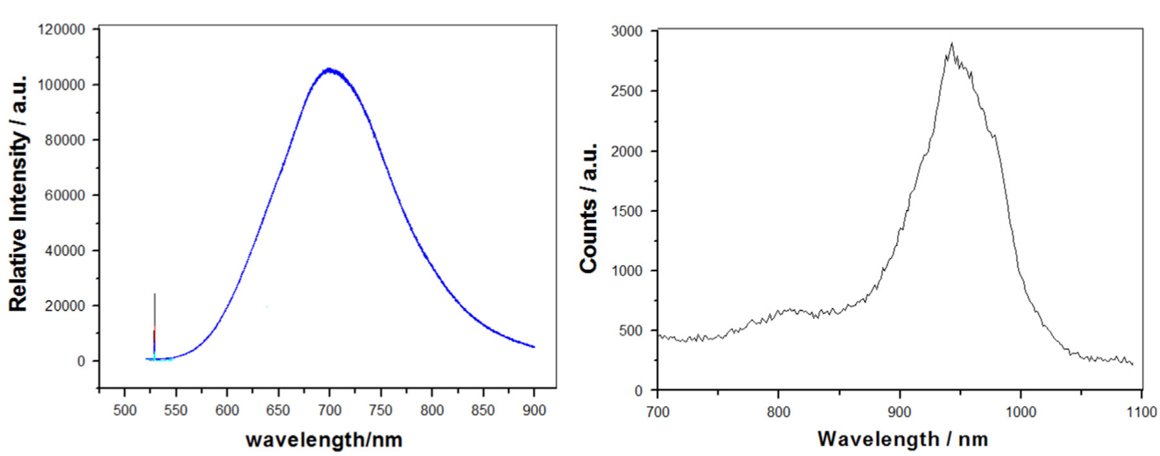

Fig. 3. PL band originated from QDs (a) the emission peak near 700 nm originated from Si QD states, (b) the emission peak near 900 nm originated from Ge QD states.

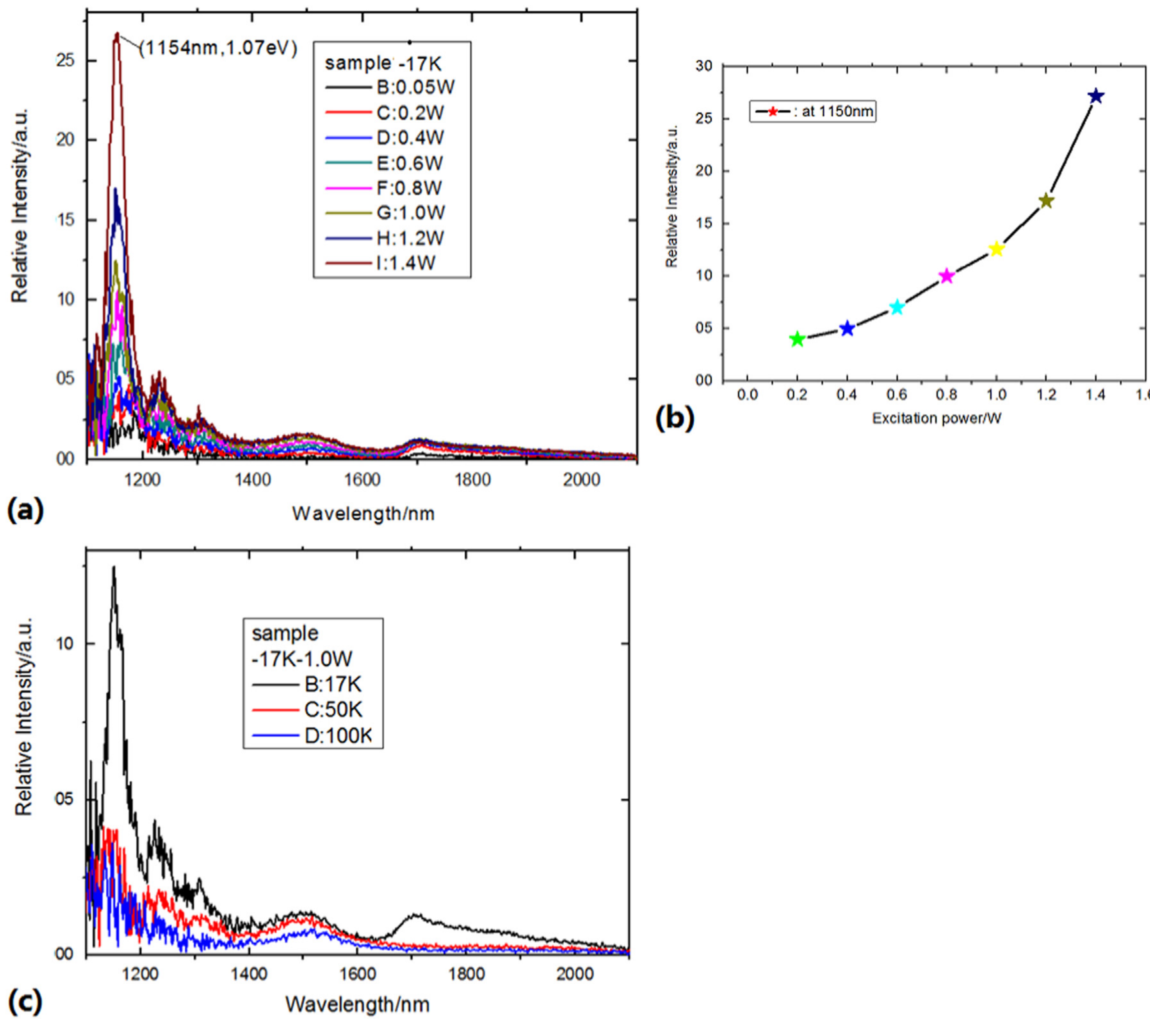

Fig. 4. (a) PL peaks on the Si nanolayers involving QDs in [100] direction measured under the 488 nm excitation in PL Systems at 17 K, in which the intensity of emission peak near 1150 nm super-linearly increases with pumping power, (b) Evolution curve of the emission intensity at 1154 nm increasing with pumping power super-linearly on the samples, (c) Change of PL spectra at different temperature with pumping power of 1 W on the samples.

the emission states.

It is interesting that the sharper enhanced PL peaks with multi-longitudinal-mode are measured at room temperature in the super-lattice structure of Si nanolayers involving Si QDs, as shown in Fig. 5, in which more peaks in multi-longitudinal-mode occur in Fig. 5(b) are related to more layers (8 layers) of the super-lattice structure, while the less peaks in Fig. 5(a) originate from the less layers (6 layers) of the super-lattice structure. It is demonstrated

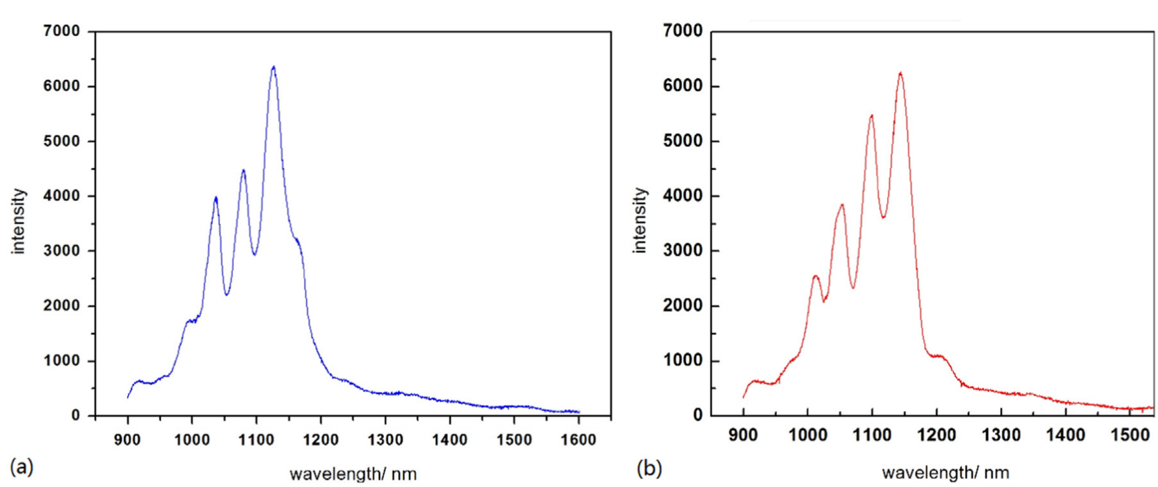

Fig. 5. PL peaks measured at room temperature in the super-lattice structure of Si-Ge layers involving QDs prepared in environment of nitrogen (a) Less peaks with multi-longitudinal-mode occurring in the structure with 6 layers of the super-lattice structure, (b) More peaks with multi-longitudinal-mode occurring in the structure with 8 layers of the super-lattice structure.

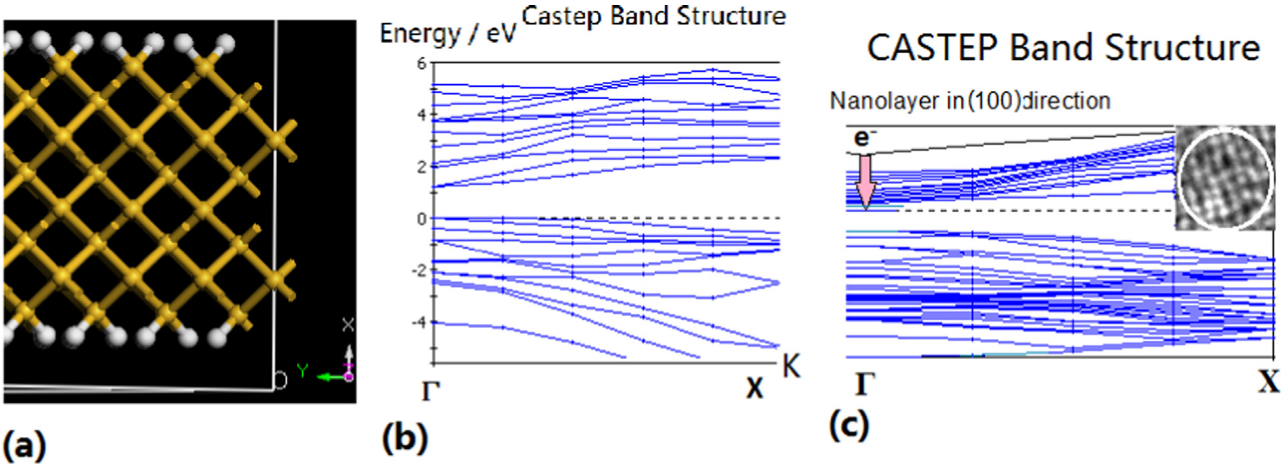

Fig. 6. Nano-layer structure of silicon (about 2 nm) (a), its energy band structure (rising of X valley of Si conduction band) (b) and their model, in which the rising states in Si QDs provide pumping levels for emission of nanolayers states at Γ point.

that more peaks with the multi-longitudinal-mode are observed in the super-lattice structure with more Si nanolayers involving Si QDs due to the quantum coupling among more quantum wells.

Some model has been chosen to simulate the experimental process. In the work, the electronic behavior is investigated by an ab initio non-relativistic quantum mechanical analysis. The DFT calculation were carried out by using the local density approximation (LDA) and non-local gradient-corrected exchange-correlation functional (GGA) for the self-consistent total energy calculation. The simulating calculation demonstrates that the conduction band valley rises in the Si QDs and the Si nanolayer structure, as shown in Fig. 6, in which Fig. 6(a) shows the Si nanolayer structure, Fig. 6(b) shows its energy band structure with rising X valley of conduction band, and Fig. 6(c) shows the electronic states structures. Here, the rising electronic states in Si nanostructures provide pumping levels for emission.

In the same way, as shown in Fig. 7(a), the emission peaks near 1400 nm in the PL spectra are measured in Ge nanostructure in [111] direction at 20 K, in which the center intensity of PL peaks increases with pumping power. And Fig. 7(b) shows the PL peak near 1550 nm measured in Ge nanostructure in [111] direction at room temperature. Here, the PL peak near 1400 nm at 20 K and the PL peak near 1550 nm at room temperature originate from the electronic states of direct band-gap in nanolayer with QD states pumping.

In Fig. 7(c), it is interesting that the sharper enhanced peaks with multi-longitudinal-mode measured in the super-lattice structure of Ge nanolayers involving QDs prepared in environment of SF_6 have super-linear evolution of emission intensity with increase of pumping power, which provide a new material on chip laser.

In the simulating calculation, Fig. 8 shows the Ge-Si layers model structure (a), its band structure (b) and its states structures of QDs and nanolayers (c), in which the valley of conduction band of germanium at L point rises to be higher than the valley of conduction band at Γ point originated from the Ge nanostructures in [111] direction after annealing to form direct band-gap structures.

A physical model of emission with three-level system is built in the Si and Ge layers involving QDs, as shown in Fig. 9, in which it is clear that the rise of X valley in Si nanolayer and L valley in Ge nanolayer forms the direct-gap levels at Γ valley near 1.1 eV and 0.8 eV respectively. The inverse population in the nanolayers states could be produced with pumping of QD states. It is noted that the lifetime of QD states is shorter than that of nanolayers due to the Heisenberg principle related to $\Delta t \sim h/\Delta E$ in the quantum confinement effect, which is suitable for pumping.

In the summary, the Si and Ge layers in the [100] and [111]

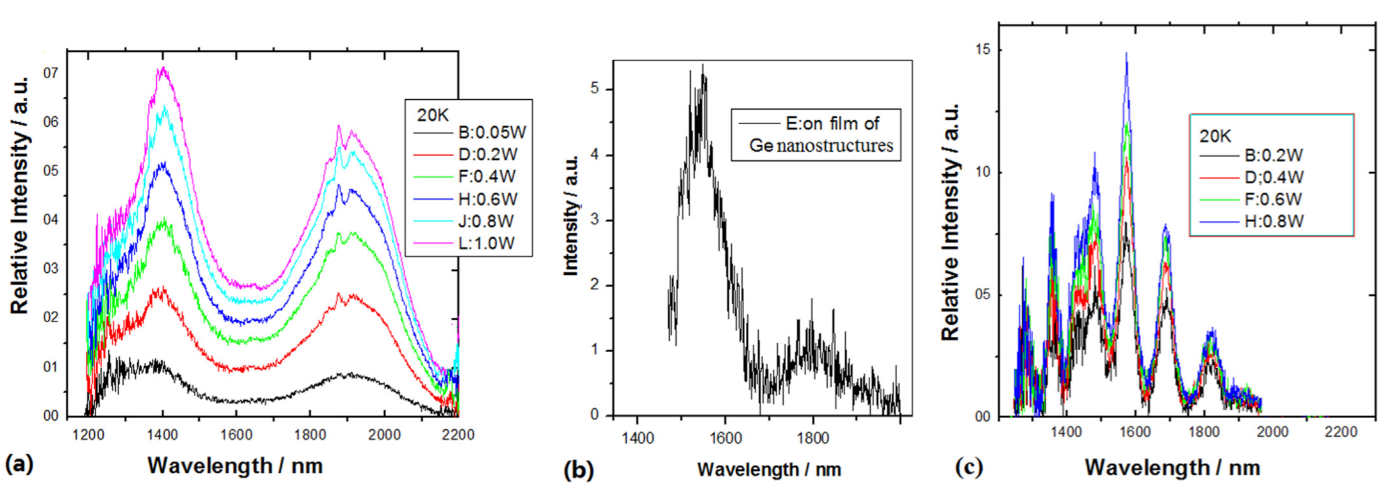

Fig. 7. PL spectra measured at 20 K in the Ge nanolayers involving Ge QDs prepared in environment of SF_6, (a) Emission peaks near 1400 nm and 1900 nm in the PL spectra measured in the Ge nanostructure in [111] direction at 20 K, in which the intensity evolution with increase of pumping power occurs; (b) PL peak near 1550 nm measured in Ge nanostructure in [111] direction at room temperature (c) PL peaks with multi-longitudinal-mode measured at 20 K in the super-lattice structure of Ge nanolayer involving QDs, in which the intensity evolution with increase of pumping power super-linearly appears.

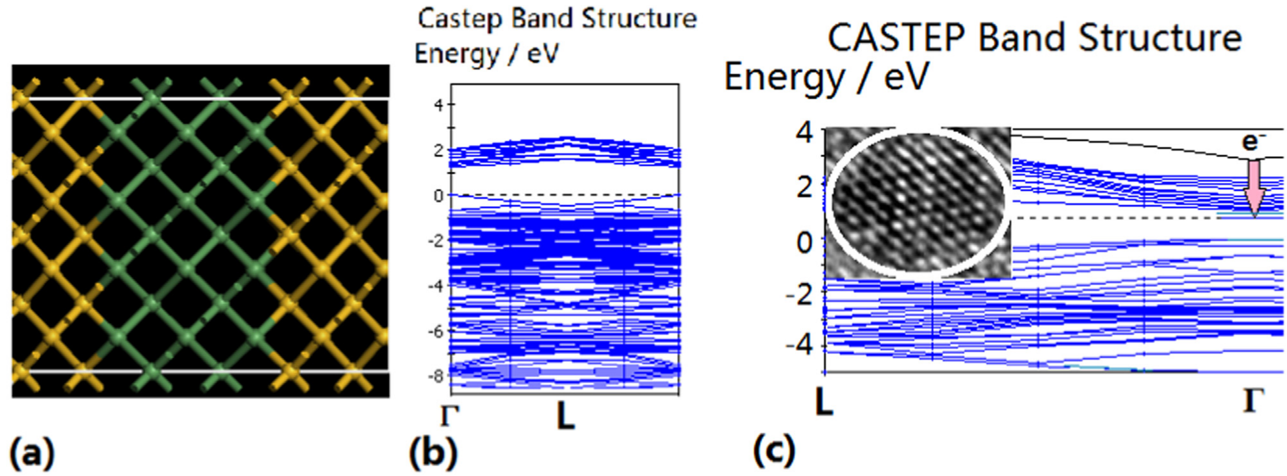

Fig. 8. (a) Sand-witch structure of Si-Ge-Si nanolayers model in simulation (b) Energy band structure of Si-Ge-Si nanolayers, in which the valley of conduction band of nanogermanium at L point rises to reach to Γ valley of conduction band (c) Electronic states model in the Ge nanostructures.

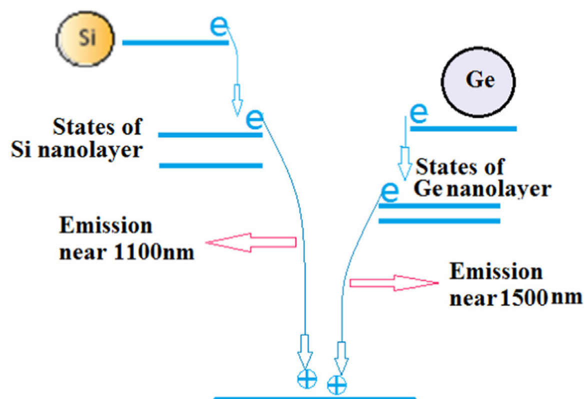

Fig. 9. Physical model of emission with three levels system built in the Si and Ge nanolayers involving QDs, in which the rise of X valley in nanosilicon and L valley in nanogermanium forms the pumping levels, and the Γ valleys of Si and Ge nanolayers states become emission levels with inverse population.

direction were fabricated by using PLD process, on which the PL emission of direct band-gap was measured at room temperature and 20 K. It is interesting that the sharper intensive peaks with multi-longitudinal-mode near 1150 nm and near 1500 nm were observed at room temperature and 20 K on the super-lattice structure of Si and Ge layers involving QDs, which have the characteristics of direct band-gap material with pumping of the QD states. The band-gap energy near 0.8 eV related to emission near 1500 nm is useful for technological application. We have built the physical model of direct band-gap emission with three-level system to explain the simulation and experimental results. It is a new road to obtain new direct band-gap emission in four-group materials and to develop Si-Ge laser on silicon chip.

Acknowledgements

This work was supported by the National Natural Science Foundation of China (Grant No.11264007, 61465003).

References

[1] R. Kirchain, L. Kimerling, A roadmap for nanophotonics, Nat. Photonics 1 (2007) 303–305.
[2] L. Pavesi, L. Dal Negro, C. Mazzoleni, G. Franzo, E. Priolo, Optical gain in silicon nanocrystals, Nature 408 (2000) 440–444.
[3] Z. Lu, D.J. Lockwood, J. Baribeau, Quantum confinement and light emission in SiO_2/Si superlattice, Nature 378 (1995) 258–260.
[4] Ming Yang, Qiang Wu, Zhandong Chen, Bin Zhang, Baiquan Tang, Jianghong Yao, Irena Drevensek-Olenik, Jingjun Xu, Generation and erasure of femtosecond laser-induced periodic surface structures on nanoparticle-covered silicon by a single laser pulse, Opt. Lett. 39 (2) (2014) 343–346.
[5] P. Chaisakul, et al., Quantum-confined Stark effect measurements in Ge/SiGe quantum-well structures, Opt. Lett. 35 (2010) 2913–2915.
[6] Y.H. Kuo, et al., Strong quantum-confined Stark effect in germanium quantum-well structures on silicon, Nature 437 (2005) 1334–1336.
[7] S. Ren, et al., Ge/SiGe quantum well waveguide modulator monolithically integrated with SOI waveguides, IEEE Photonics Technol. Lett. 24 (2012) 461–463.
[8] S. Das, et al., Electroluminescence and charge storage characteristics of quantum confined germanium nanocrystals, J. Appl. Phys. 110 (2011) 024310.
[9] Z. Zhang, C. Zeng, H. Zhang, D. Li, G. Gao, Q. Huang, Y. Wang, J. Yu, J. Xia, Single-mode emission from Ge quantum dots in photonic crystal nanobeam cavity, IEEE Photonics Technol. Lett. 27 (2015) 1026–1029.
[10] W.Q. Huang, Z.M. Huang, H.Q. Chen, X.J. Miao, Electronic states and curved surface effect of silicon quantum dots, Appl. Phys. Let. 101 (2012) 171601.
[11] W.Q. Huang, S.R. Liu, Z.M. Huang, T.G. Dong, G. Wang, C.J. Qin, Magic electron affection in preparation process of silicon nanocrystal, Nat. Sci. Rep. 4 (9932) (2015) 09932, http://dx.doi.org/10.1038/srep.
[12] M. El Kurdi, T. Kociniewski, T.P. Ngo, J. Boulmer, D. Debarre, P. Boucaud, J. F. Damlencourt, O. Kermarrec, D. Bensahel, Enhanced photoluminescence of heavily n-doped germanium, Appl. Phys. Lett. 94 (2009) 191107.
[13] X.C. Sun, J.F. Liu, Lionel C. Kimerling, Jurgen Michel, Direct gap photoluminescence of n-type tensile-strained Ge-on-Si, Appl. Phys. Lett. 95 (2009) 011911.
[14] M. El Kurdi, H. Bertin, E. Martincic, M. De Kersauson, G. Fishman, S. Sauvage, A. Bosseboeuf, P. Boucaud, Control of direct band gap emission of bulk germanium by mechanical tensile strain, Appl. Phys. Lett. 96 (2010) 041909.
[15] H. Tahini, A. Chroneos, R.W. Grimes, U. Schwingenschlog, A. Dimoulas, Strain-induced changes to the electronic structure of germanium, J. Phys. Condens. Matter 24 (2012) 195802.
[16] W.Q. Huang, S.R. Liu, Z.M. Huang, T.G. Dong, G. Wang, C.J. Qin, Silicon nanocrystal growth under irradiation of electron beam, Sci. Rep. 5 (2015) 16682.